J. Membrane Biol. 158, 59–67 (1997)

The Journal of
Membrane
Biology

Differential Effect of High Extracellular Ca^{2+} on K^+ and Cl^- Conductances in Murine Osteoclasts

T. Shibata[1], **H. Sakai**[1], **F. Nakamura**[1], **A. Shioi**[2], **M. Kuno**[1]

Departments of Physiology[1] and Internal Medicine[2], Osaka City University Medical School, Abeno-ku, Osaka, 545, Japan

Received: 28 May 1996/Revised: 28 January 1997

Abstract. Effects of the extracellular Ca^{2+} concentration ($[Ca^{2+}]_o$) on whole cell membrane currents were examined in mouse osteoclastic cells generated from bone marrow/stromal cell coculture. The major resting conductance in the presence of 1 mM Ca^{2+} was mediated by a Ba^{2+}-sensitive, inwardly rectifying K^+ (IR_K) current. A rise in $[Ca^{2+}]_o$ (5–40 mM) inhibited the IR_K current and activated an 4,4′-diisothiocyano-2,2′-stilbenedisulfonate (DIDS)-sensitive, outwardly rectifying Cl^- (OR_{Cl}) current. The activation of the OR_{Cl} current developed slowly and needed higher $[Ca^{2+}]_o$ than that required to inhibit the IR_K current. The inhibition of the IR_K current consisted of two components, initial and subsequent late phases. The initial inhibition was not affected by intracellular application of guanosine 5′-O-(3-thiotriphosphate) (GTPγS) or guanosine 5′-O-(2-thiodiphosphate) (GDPβS). The late inhibition, however, was enhanced by GTPγS and attenuated by GDPβS, suggesting that GTP-binding proteins mediate this inhibition. The activation of the OR_{Cl} current was suppressed by pretreatment with pertussis toxin, but not potentiated by GTPγS. An increase in intracellular Ca^{2+} level neither reduced the IR_K current nor activated the OR_{Cl} current. Staurosporine, an inhibitor for protein kinase C, did not modulate the $[Ca^{2+}]_o$-induced changes in the IR_K and OR_{Cl} conductances. These results suggest that high $[Ca^{2+}]_o$ had a dual action on the membrane conductance of osteoclasts, an inhibition of an IR_K conductance and an activation of an OR_{Cl} conductance. The two conductances modulated by $[Ca^{2+}]_o$ may be involved in different phases of bone resorption because they differed in Ca^{2+} sensitivity, temporal patterns of changes and regulatory mechanisms.

Key words: Osteoclast — Extracellular Ca^{2+} — Cl^- current — K^+ current — G proteins

Correspondence to: M. Kuno

Introduction

Osteoclasts play an important role in bone remodeling and Ca^{2+} homeostasis by resorbing calcified tissues via acid secretion. At the resorptive pit, osteoclasts are exposed to high concentrations of extracellular Ca^{2+} ($[Ca^{2+}]_o$). An elevation of $[Ca^{2+}]_o$ leads to cell-retraction, de-adhesion [17, 19, 43] and a reduced secretion of resorptive enzymes [20, 43], resulting in inhibition of bone resorption [9, 17, 19, 41]. Thus $[Ca^{2+}]_o$ works as an exquisite negative feedback signal in the regulation of osteoclastic functions. As acid secretion of osteoclasts is considered to be mediated by electrogenic H^+-ATPase [6, 11, 39] and depends on Cl^- transport [7, 11, 18], membrane conductance would be expected to affect osteoclast activity. An elevation of $[Ca^{2+}]_o$ has been reported to inhibit K^+ channels, either inwardly rectifying K^+ (IR_K) [3, 12, 21, 40] or outwardly rectifying K^+ (OR_K) channels [3] in freshly isolated osteoclasts, but the role of ionic conductances of osteoclasts in response to changes in $[Ca^{2+}]_o$ remains to be defined.

Certain cells, which are involved in bodily Ca^{2+} homeostasis, sense $[Ca^{2+}]_o$ and change their activity. The cell surface Ca^{2+} receptor on parathyroid cells have been sequenced and found to be coupled to a GTP-binding protein (G-protein) [8]. Activation of the Ca^{2+} receptor generates intracellular signals through the receptor-phospholipase C pathway, resulting in an elevated intracellular Ca^{2+} concentration ($[Ca^{2+}]_i$) and diacylglycerol level [14, 21, 23, 30]. Osteoclasts are distinct in sensing changes in the milimolar range $[Ca^{2+}]_o$. Activity of osteoclasts is considered to be regulated by a low-affinity receptorlike mechanism sensing $[Ca^{2+}]_o$ [17, 19, 42], but the cell machinery for responding to high $[Ca^{2+}]_o$ is yet to be identified on the molecular level. An elevation of $[Ca^{2+}]_o$ increases $[Ca^{2+}]_i$ due to both Ca^{2+} release from the internal stores and Ca^{2+} influx through the plasma membrane in osteoclasts as well [17, 41]. Protein kinase C (PKC) is also suggested to act as an intracellular sig-

nal, since PKC isozyme is translocated from the cytosolic to the particulate fraction by elevated $[Ca^{2+}]_o$ [37]. However, little is known on the intracellular signaling pathways involved in osteoclastic functions regulated by $[Ca^{2+}]_o$.

Osteoclasts are of hematopoietic origin. A coculture of mouse bone marrow cells with osteoblastic stromal cells in the presence of a biologically active form of vitamin D_3 ($1\alpha,25(OH)_2D_3$) produces multinucleated cells that have the characteristics of osteoclasts, including a unique morphology, tartate resistant acid phosphatase (TRAP) activity, expression of calcitonin receptors and bone resorptive ability [1, 5, 28, 35, 36]. This bone marrow culture system provides a large number of mammalian osteoclasts, enabling extensive studies of osteoclastic functions to be pursued. This study was aimed at investigating the effects of $[Ca^{2+}]_o$ on the membrane conductance of the in vitro-generated osteoclasts. We found that an elevation of $[Ca^{2+}]_o$ (~40 mM) had a dual action on the membrane conductance, with an inhibition of an IR_K current followed by a slow activation of an outwardly rectifying Cl^- (OR_{Cl}) current. The changes in the two conductances in response to an increase in $[Ca^{2+}]_o$ differed in the temporal patterns, dose-dependencies and regulatory mechanisms, thereby suggesting that the IR_K and OR_{Cl} currents are involved in different phases of bone resorption. A preliminary account has been made [27].

Materials and Methods

Cell Culture

Osteoclastic cells were generated from coculture of bone marrow cells of male, 5–8-week-old mice (C3H/HEN) with a marrow-derived stromal cell line (ST2) (Riken Cell Bank, Tsukuba, Japan) following the method previously described [28]. The mice were killed by cervical dislocation. Bone marrow cells were obtained from the femurs and tibias, centrifuged at 1500 rpm for 7 min at 4°C in α-MEM supplemented with 10% fetal calf serum (FCS), streptomycin (0.1 mg ml^{-1}) and penicillin (100 U ml^{-1}). After incubation at 37°C in a 95% air-5% CO_2 atmosphere overnight, nonadherent cells were collected, centrifuged at 800 × *g* at 4°C for 7 min and then incubated in the phosphate-buffered saline containing 0.02% pronase and 1.5 mM EDTA for 15 min at 37°C. The pronase reaction was stopped by heat-inactivated horse serum (0.2 ml/10 ml pronase solution), and the cell suspension was layered on ice-cold horse serum. After 15 min of sedimentation at unit gravity for 15 min on the ice-cold horse serum, the uppermost part of the layers were collected, transferred on cold horse serum and then centrifuged at 1200 × *g* at 4°C for 10 min. The bone marrow cell pellet was suspended in fresh α-MEM supplemented with 10% FCS at 1×10^6 cells/ml and cocultured with ST2 cells (1×10^5 cells/ml) in the presence of 10^{-8} M $1\alpha,25(OH)_2D_3$ (Duphar) and 10^{-7} M dexamethasone at 37°C in a 95% air-5% CO_2 atmosphere. Total medium was changed twice a week. Multinucleated cells with a unique osteoclastic morphology and TRAP activity were identified at 5–7 days after the start of coculture and were maintained for up to 18 days. ST2 cells were removed by incubation with 0.1% collagenase/0.1% bovine serum albumin (BSA) in α-MEM for 20 min to 2 hrs at 37°C before recordings were made.

Electrophysiological Recordings

Current signals were recorded using the whole cell clamp configuration at room temperature (20–24°C). The reference electrode was an Ag-AgCl wire connected to the bath solution through a Ringer-agar bridge. The standard pipette solution contained (in mM): 150 K-glutamate, 7 $MgCl_2$, 1 EGTA, 1 Na_2ATP, 10 HEPES-KOH (pH 7.3). In some experiments, K-glutamate was replaced by CsCl, Cs-methanesulfonate or a mixture of both, to block K^+ currents and to produce intracellular solutions containing various concentrations of Cl^-. To investigate effects of the elevated intracellular Ca^{2+} levels on current activities, the pipette solutions containing 1–10 μM Ca^{2+} were prepared with the Ca^{2+}-EGTA mixture [22]. The standard external solution contained (in mM): 145 NaCl, 5 KCl, 1 $CaCl_2$, 1 $MgCl_2$, 10 glucose, 0.1% BSA and 10 HEPES-NaOH (pH = 7.3). The high Ca^{2+} (5–40 mM) or high K^+ (30 and 150 mM) solutions were made by replacing NaCl with $CaCl_2$ or KCl to compensate for osmolarity. Pipette resistance ranged between 5–8 MΩ. The series resistance compensation (~70%) was conducted to reduce the voltage error. The zero current potential before formation of the gigaseal was taken as 0 mV. Data without an adequate voltage control in some cells with large currents were not quantitatively analyzed in this study.

Currents were recorded by an amplifier (Axopatch 200A). After digitizing at 1 kHz through a analog-digital converter (Digidata 1200), data were stored and analyzed by a personal computer (pClamp 6.02). Whole cell capacitance was estimated using the capacitance compensation circuit of the amplifier (108 ± 54 pF, $n = 111$; min–max, 33–302 pF). Voltage ramps (0.4–1 mV $msec^{-1}$ from −120 to 120 mV) were applied at the holding potential of 0 or −60 mV. Leak current was determined from the linear portion of the current-voltage (*I–V*) relation when either IR current or OR current was absent or when the currents were eliminated by the blockers. The IR and OR conductances were obtained from the *I–V* relation between −100 and −80 mV and between +80 and +100 mV, respectively, after subtraction of the leak current. Within this voltage range, the conductance estimated from the voltage ramp method was almost identical to that obtained by measuring the peak current amplitude evoked by voltage steps: the conductance estimated from the voltage ramp method was 103 ± 10% ($n = 17$) of that estimated from voltage-steps. All data were expressed as mean ± SD.

Identification of Cells

Currents were recorded from cells with three or more nuclei. Most of cells used for this study had a unique morphology similar to the ''spread type'' of freshly isolated osteoclasts with a flattened cell body and developed lamellipodia and retraction fibers [2, 12]. TRAP activity of the cells used for recordings was confirmed by a staining kit in the early part of experiments.

Chemicals

Unless otherwise specified, all chemicals were obtained from Sigma. Pertussis toxin (PTX) was obtained from Kaken Pharmac.

Results

The Resting Conductance

A major resting current of in vitro-generated osteoclasts was an inwardly rectifying (IR) current activated by hy-

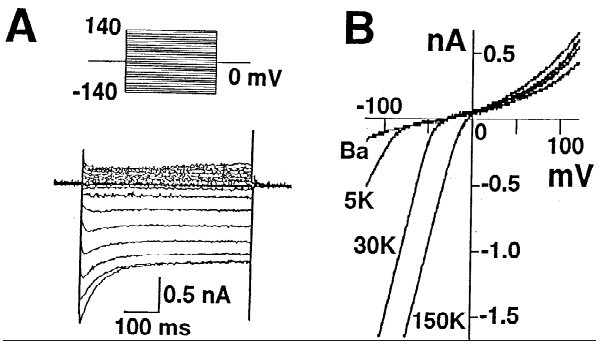

Fig. 1. Inwardly rectifying K^+ (IR_K) current in the resting state. Whole-cell current was recorded in the standard extracellular solution containing 1 mM Ca^{2+}. (*A*) A family of currents evoked by step voltage pulses from −140 to +140 mV in ±10 mV increments applied at a holding potential of 0 mV. (*B*) *I–V* relations obtained by voltage ramps in a cell which was subsequently perfused with solutions containing 5, 30 and 150 mM K^+. The IR_K current was blocked by 1 mM Ba^{2+}. Leak current was not subtracted in *A* and *B*. The pipette solution contained K-glutamate in this and later figures unless described otherwise.

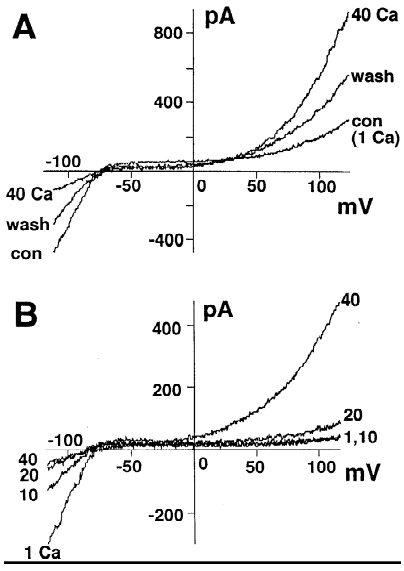

Fig. 2. Effects of $[Ca^{2+}]_o$ on whole cell current. (*A*) superimposed *I–V* relations obtained by voltage ramps applied at a holding potential of 0 mV, before and 5 min after application of 40 mM Ca^{2+}. Washout of 40 mM Ca^{2+} tended to recover the control levels (*B*) Superimposed *I–V* relations in a cell subsequently perfused with 1, 10, 20 and 40 mM Ca^{2+}. The data were obtained when the OR_{Cl} current reached to the maximum (within 5–10 min following the application of the $[Ca^{2+}]_o$). *A* and *B* were obtained from different cells. Leak current was subtracted.

perpolarizing pulses. Figure 1*A* shows representative membrane currents in a cell bathed in the standard Ringer solution containing 1 mM Ca^{2+}. The outward conductance was much smaller than the inward conductance in most cells. The mean inward conductance was 85.0 ± 52.4 (min–max; 8–232) pS/pF and the mean outward conductance was 15.0 ± 18.2 (0.8–83.6) pS/pF in 36 cells. The great variety of the IR conductance normalized by cell capacitance shows that cells with similar size and morphological appearance had a very large range of IR conductance. Factors other than cell size seem to cause this variation. Sizable outward currents were occasionally recorded, but were not characterized because of the low incidence.

The IR current was augmented by increasing the extracellular K^+ concentration ($[K^+]_o$) and eliminated by 1 mM Ba^{2+} (Fig. 1*B*). The reversal potential of the IR current, estimated from crossings between *I–V* curves with and without Ba^{2+}, was positively shifted by increasing the $[K^+]_o$. The mean and SD of the reversal potentials were −74.4 ± 3.1 mV ($n = 5$), −40.3 ± 6.8 mV ($n = 5$) and 8.4 ± 6.9 mV ($n = 5$) with 5, 30 and 150 mM K^+, respectively. A least squares fit for reversal potentials to $[K^+]_o$ on a semilogarithmic scale had a slope of 56 mV per tenfold change in $[K^+]_o$, indicating that the IR current was mediated by K^+ (IR_K).

High $[Ca^{2+}]_o$ Inhibits the Inwardly Rectifying K^+ (IR_K) Current and Activates an Outwardly Rectifying (OR) Current

Figure 2 illustrates the typical effects of an increase in $[Ca^{2+}]_o$ on the membrane conductance. The *I–V* relations were obtained by voltage ramps applied at a holding potential of 0 mV when $[Ca^{2+}]_o$ was increased from 1 to 40 mM. An elevation of $[Ca^{2+}]_o$ reduced the IR_K current and increased an outwardly rectifying (OR) current, and the conductances tended to return to the control levels following the washout of high Ca^{2+} (Fig. 2*A*). Outward currents at a limited range of voltage positive to the reversal potential of the IR_K current were often slightly reduced by high $[Ca^{2+}]_o$. This reduction is probably due to a decrease in the negative conductance region of the IR_K current, as reported in freshly isolated osteoclasts [3, 40].

Inhibition of the IR_K current was made evident by application of 10 mM Ca^{2+} while activation of the OR current needed higher $[Ca^{2+}]_o$ (Fig. 2*B*). Dose-response relations for the effects of $[Ca^{2+}]_o$ on the IR and OR conductances were summarized in Fig. 3. Data were obtained by voltage ramps applied at a holding potential of 0 mV when the effect of $[Ca^{2+}]_o$ was maximal. The IR_K conductance was normalized by that with 1 mM Ca^{2+} and the OR conductance, by the maximum amplitude with 40 mM Ca^{2+}. It is noted that the curve for the OR current was steep at higher than 20 mM Ca^{2+}, while inhibition of the IR_K current was almost linear over $[Ca^{2+}]_o$ up to 40 mM on a semilogarithmic scale. The resting potential of osteoclasts has been reported to switch two levels, more positive than −20 mV and more negative than −60 mV [12, 32, 33, 40]. The IR_K current was reduced by 40 mM Ca^{2+} to 33 ± 18% of controls (*n*

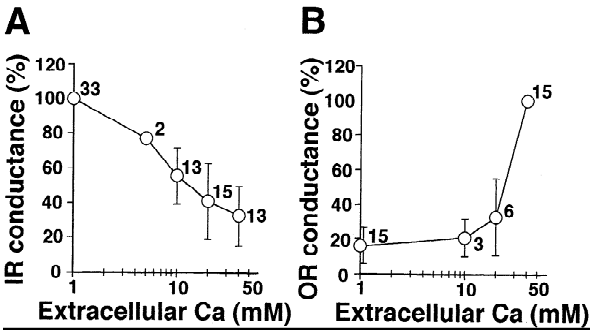

Fig. 3. Dose-response relationships of $[Ca^{2+}]_o$-induced changes in membrane conductances. Magnitudes of IR (*A*) and OR (*B*) currents were plotted against $[Ca^{2+}]_o$ on a semilogarithmic scale. (*A*) The IR conductance at various $[Ca^{2+}]_o$ was expressed as percentage of that with 1 mM Ca^{2+}. (*B*) The OR conductance was expressed as percentage of that with 40 mM Ca^{2+}. Data were obtained at times when the effect of $[Ca^{2+}]_o$ was maximal and expressed as mean ± SD. Number of cells tested is given with data point.

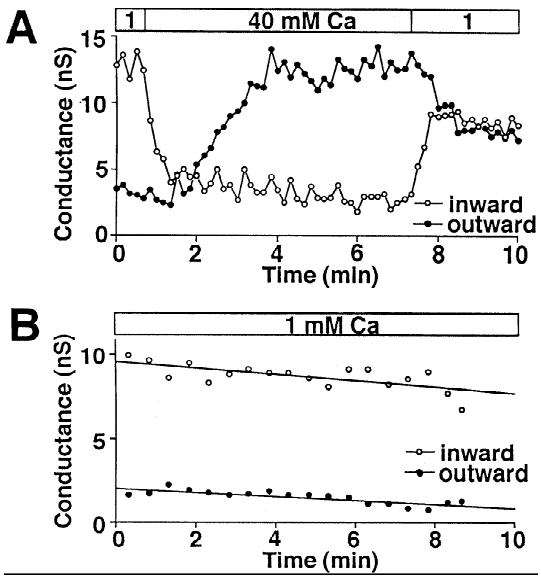

Fig. 4. Time courses of $[Ca^{2+}]_o$-induced changes in membrane conductances. Open and closed circles represent IR and OR conductances, respectively. (*A*) Conductances of a cell when $[Ca^{2+}]_o$ was changed from 1 to 40 mM and then returned to 1 mM. (*B*) Conductances of a cell during recordings without change in $[Ca^{2+}]_o$. *A* and *B* were obtained from different cells at a holding potential of 0 mV.

= 13) at a holding potential of 0 mV and 30 ± 22% (n = 8) at −60 mV. The OR current was also activated at both 0 and −60 mV. Thus the changes in the two conductances in response to an increase in $[Ca^{2+}]_o$ were induced independently of the holding potential. Forty mM Ca^{2+} inhibited the IR_K current in most cells tested and activated the outward current in 25 out of 41 cells within 2 min following the start of perfusion of the high Ca^{2+} solution.

Figure 4 shows the time courses of changes in the IR and OR conductances when $[Ca^{2+}]_o$ was increased from 1 to 40 mM. The cell was perfused with the high Ca^{2+} solution at about 0.1 ml sec^{-1} (volume of the recording chamber; 2 ml). The IR_K conductance rapidly decreased but activation of the OR conductance developed more slowly (Fig. 4*A*). In seven cells associated with changes in the two conductances by 40 mM Ca^{2+}, the time required to induce half maximal inhibition of the IR_K current was 35 ± 11 sec (n = 7), and the time to induce half-maximal activation of the OR current was 114 ± 22 sec (n = 7). The time may include lag due to bath perfusion (10–30 sec). Following the washout of high $[Ca^{2+}]_o$, the IR_K current rapidly increased to 60–75% of controls within 2 min, but did not fully recover after a long exposure to high Ca^{2+}. This might be partially due to rundown independent of $[Ca^{2+}]_o$ (2.9 ± 1.8%/min, n = 16) (Fig. 4*B*). Recovery of the OR current was slower. Following the washout, the OR current decreased by 30–80% of the maximum within 10 min. In three cells which were exposed to 40 mM Ca^{2+} for longer than 20 min, the OR current did not decrease by the washout over a recording period of up to 10 min. Thus, changes in the two conductances by an increase in $[Ca^{2+}]_o$ had different temporal patterns.

The OR Current Activated by High $[Ca^{2+}]_o$ is Mediated by Cl^-

The OR current activated by $[Ca^{2+}]_o$ was rapidly activated by depolarization and inactivation was negligible during voltage pulses of 500 msec (Fig. 5*A*). The OR current was blocked by a Cl^- channel blocker, 4,4′-diisothiocyano-2,2′-stilbenedisulfonate (DIDS) (50–100 μM) (Fig. 5*B*) in all 7 cells tested. In addition, the OR current was activated by high Ca^{2+} even with Cs^+ as a substitute for K^+ in the intracellular solution (Fig. 5*C*). With pipette solutions containing Cs^+ and different concentrations of Cl^-, whole cell currents were recorded in the presence of 1 and 40 mM $[Ca^{2+}]_o$. Reversal potentials of the difference current were positively shifted by increasing the intracellular Cl^- concentration ($[Cl^-]_i$) and a least squares fit on a semilogarithmic scale had a slope of 51 mV per tenfold change in $[Cl^-]_i$ (Fig. 5*D*). These results suggest that Cl^- is a major ion carrier for the OR current activated by high $[Ca^{2+}]_o$ (OR_{Cl}).

Intracellular Signaling Pathways Involved in the $[Ca^{2+}]_o$-induced Changes in the Membrane Conductances

We examined the effects of pertussis toxin (PTX) and unhydrolyzable analogues for GTP and GDP, guanosine 5′-O-(3-thiotriphosphate) (GTPγS) and guanosine 5′-O-

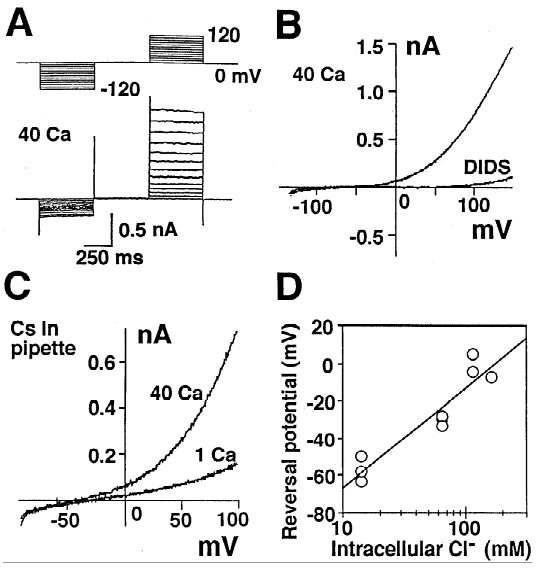

Fig. 5. OR current activated by high $[Ca^{2+}]_o$ is mediated by Cl^-. (*A*) A family of currents evoked by step voltage pulses in ±10 mV increments applied at a holding potential of 0 mV in the presence of 40 mM Ca^{2+}. (*B*) Superimposed *I–V* relations obtained by applying voltage ramps in the presence and absence of a Cl^- channel blocker, DIDS (100 μM). (*C*) Superimposed *I–V* relations in the presence of 1 and 40 mM Ca^{2+} recorded with 150 mM Cs-methanesulfonate in the pipette. The leak current was subtracted in B and C, but not in *A*. (*D*) Semilogarithmic plot of the reversal potential of the Ca^{2+}-activated OR current against $[Cl^-]_i$. Intracellular solutions contained Cs^+ and different concentrations of Cl^-. The line indicate a least squares fit for data with a slope of 51 mV per tenfold change in $[Cl^-]_i$.

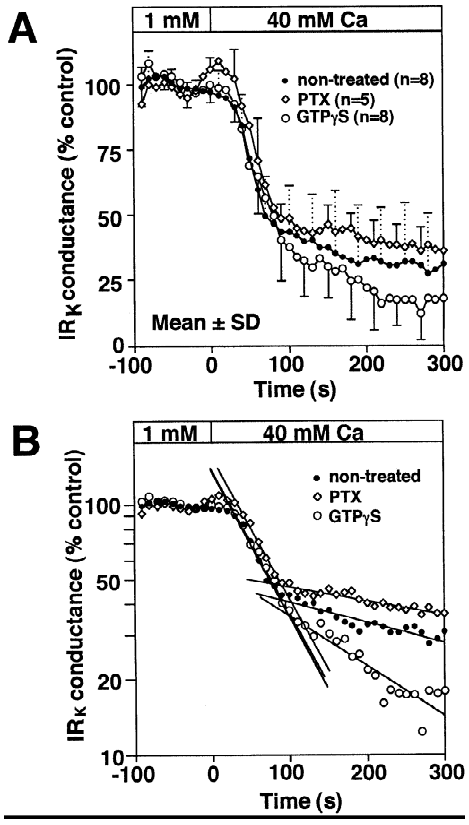

Fig. 6. Effects of pertussis toxin (PTX) and GTPγS on $[Ca^{2+}]_o$-induced inhibition of IR_K conductance. (*A*) Time courses of inhibition of IR_K conductance by 40 mM Ca^{2+}. The IR_K conductances were expressed as percentage of the 10 averaged control responses obtained in the presence of 1 mM Ca^{2+}. Each point indicates mean magnitudes in non-treated (closed circles), PTX-treated (diamonds) and intracellular GTPγS-treated (open circles) cells. SD was attached to every three points. (*B*) Semilogarithmic plot of the averaged time courses. Lines indicate regressions fitted to data during the initial (30–100 sec) and late (100–300 sec) phases. In PTX-treated cells, cells were incubated with 500 ng ml^{-1} PTX for 2–7.5 hr at 37°C. GTPγS (100 μM) was added to the pipette solution. Cells were held at −60 mV during the entire course of experiments.

(2-thiodiphosphate) (GDPβS), on the changes in the membrane conductance by elevated $[Ca^{2+}]_o$, since the Ca^{2+}-receptor in parathyroid cells links with G-proteins [8, 21]. Figure 6*A* illustrates averaged time courses of inhibition of the IR_K conductance by 40 mM Ca^{2+} in nontreated ($n = 8$), PTX-treated ($n = 5$) and GTPγS-treated ($n = 8$) cells at a holding potential of −60 mV. Data are expressed as percentage of the mean of 10 successive control conductances before application of high $[Ca^{2+}]_o$ in each cell. The control IR_K conductances were not significantly different among the three groups. Semilogarithmic plots fitted by linear regressions manifest two components of the inhibition, an initial phase that was completed within 100 sec and a subsequent late phase (Fig. 6*B*). There was no difference in the initial inhibition among the three groups, indicating that the initial phase was independent of actions via G-proteins. Rate of the late inhibition, expressed as a change of fraction of the control per min (Δ%/min), was 6.0 ± 3.0%/min ($n = 8$) in nontreated cells and 8.8 ± 2.8%/min ($n = 8$) in GTPγS-treated cells. In addition, with the pipette solution containing GDPβS (200–500 μM), the initial inhibition was unaffected and the late inhibition was 0.8± 0.9%/min ($n = 4$). The late inhibition was significantly enhanced in GTPγS-treated cells ($P < 0.1$, Student *t*-test) and attenuated in GDPβS-treated cells ($P < 0.01$), suggesting involvement of pathways mediated by G-proteins in the inhibitory process. The late inhibition in PTX-treated cells was 3.6 ± 3.4%/min ($n = 5$), smaller than that in non-treated cells on the average, but the suppression was not significant ($P = 0.2$).

Figure 7 shows the averaged time courses of Ca^{2+} (40 mM)-induced changes in the OR_{Cl} conductance in non-treated ($n = 8$), PTX-treated ($n = 6$) and GTPγS-treated ($n = 10$) cells. Although the magnitude of the OR_{Cl} current activated by high $[Ca^{2+}]_o$ varied

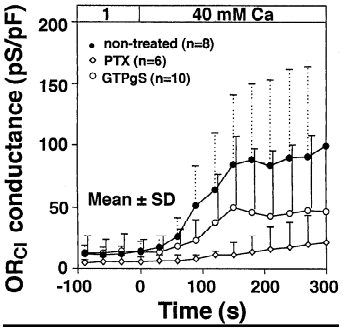

Fig. 7. Effects of PTX and GTPγS on OR_{Cl} conductance activated by high $[Ca^{2+}]_o$. Time courses of changes in OR_{Cl} conductance by 40 mM Ca^{2+} in non-treated (closed circles), PTX (500 ng/ml)-treated (diamonds) and intracellular GTPγS (100 μM)-treated (open circles) cells. Each point indicates mean OR_{Cl} conductance normalized by the cell capacitance. The attached bar indicates SD. Cells were held at −60 mV during the entire course of experiments.

among cells, the mean conductance started to increase within 100 sec in non-treated cells (closed circles). In PTX-treated cells (diamonds), the OR_{Cl} current was negligible at 100 sec and only a small increase appeared later. At 200–300 sec, the OR_{Cl} conductance was 18 ± 22 pS/pF ($n = 6$) in PTX-treated cells, which was significantly smaller ($P < 0.05$) than that in non-treated cells (98 ± 71 pS/pF; $n = 8$). However, the OR_{Cl} current was not potentiated in GTPγS-treated cells (48 ± 54 pS/pF; $n = 10$) and intracellular GTPγS (100 μM) induced the OR_{Cl} current only in one of 6 cells within 5 to 10 min following the formation of the whole cell configuration.

A rise in $[Ca^{2+}]_o$ leads to elevation of $[Ca^{2+}]_i$ [5, 17, 19, 26, 41] and translocation of PKC [38]. Neither decline of the IR_K current nor activation of the OR_{Cl} current was observed for 5–10 min following the rupture of the patch membrane to form the whole cell configuration in 7 cells with 1 μM Ca^{2+} in the intracellular solution and in 6 cells with 10 μM Ca^{2+}. An application of a Ca^{2+}-ionophore, ionomycin (1 μM) also did not activate the OR_{Cl} current within 2 min. Thus an elevation of $[Ca^{2+}]_i$ did not seem to be a sole and sufficient trigger for inhibition of the IR_K current and activation of the OR_{Cl} current. In addition, the OR_{Cl} current was not activated by 100 nM phorbol 12-myristate 13-acetate (PMA), a PKC activator ($n = 8$). Addition of PMA (100 nM) reduced the IR_K current by 8.4 ± 3.1%/min ($n = 5$), but the reduction was not significantly inhibited by 1 nM staurosporine, a PKC inhibitor. Pretreatment for 20 min with 1 nM staurosporine did not affect the changes in conductances caused by 40 mM $[Ca^{2+}]_o$: the OR_{Cl} current was 85 ± 87 pS/pF ($n = 6$) at 200–300 sec and the late inhibition of the IR_K current was 5.4 ± 3.5/min ($n = 8$), not significantly different from those in non-treated cells.

Discussion

The present study revealed that the IR_K conductance was a major resting conductance in osteoclasts generated from bone marrow/stromal cell coculture. The IR_K current observed in this study had characteristics in common with those in many cell types including mammalian [12, 32, 40] and avian [24] freshly isolated osteoclasts, such as sensitivity to Ba^{2+}, voltage-dependent inactivation and a negative conductance region at potentials positive to the reversal-potential.

Two Phases of Inhibition of the IR_K Current by High $[Ca^{2+}]_o$

During bone resorption, $[Ca^{2+}]_o$ in the resorptive pit is estimated to increase to 40 mM [31]. The $[Ca^{2+}]_o$ dose-dependently suppresses resorptive activity by causing retraction and de-adhesion of osteoclasts [9, 17, 19, 41] and by reducing resorptive enzymes [20, 43]. An elevation of $[Ca^{2+}]_o$ inhibited the IR_K current in freshly isolated osteoclasts [3, 12, 40]. A reversible inhibition of the IR_K current by high $[Ca^{2+}]_o$ was observed in the present study as well. At 40 mM Ca^{2+}, the IR_K conductance was reduced to approximately one third of that of the controls, similar to the extent of inhibition in rabbit osteoclasts [40]. The Ca^{2+}-induced inhibition described herein consisted of two components, that is, an initial phase that was completed within 100 sec, including lag due to bath perfusion, and a subsequent late phase. The extent of the late inhibition was varied among cells (6.0 ± 3.0%/min, $n = 8$), but significantly greater than the Ca^{2+}-independent rundown (2.8 ± 1.8%/min, $n = 16$) ($P < 0.005$), so that both phases of inhibition were triggered by a rise in $[Ca^{2+}]_o$. The two-phase reduction of IR_K current by high $[Ca^{2+}]_o$ has not been described in freshly isolated osteoclasts.

Activation of the OR_{Cl} Current by High $[Ca^{2+}]_o$

The present study provides the first electrophysiological evidence for a stimulatory action of $[Ca^{2+}]_o$ on Cl^- currents in osteoclasts. When compared to the inhibition of the IR_K current, a longer time and higher $[Ca^{2+}]_o$ were needed to activate the OR_{Cl} current. Washout of the high $[Ca^{2+}]_o$ tended to reduce the OR_{Cl} current more slowly than the recovery of the IR_K current, thereby suggesting that different mechanisms are responsible for the changes in the two conductances in response to an increase in $[Ca^{2+}]_o$. We cannot currently explain why the OR_{Cl} current activated by high $[Ca^{2+}]_o$ has not been detected in freshly isolated osteoclasts [3, 12, 40]. Expression of ion channels or intracellular machinery involved in the $[Ca^{2+}]_o$-induced responses may differ between freshly isolated and in vitro-generated osteoclasts.

Involvements of G-proteins in the $[Ca^{2+}]_o$-induced Changes in the Membrane Conductances

The cell surface Ca^{2+} receptor on parathyroid cells has been sequenced and was found to be a G-protein coupled receptor [8]. As intracellular application of GTPγS suppressed the IR_K current [4] and made the $[Ca^{2+}]_o$-induced inhibition of the IR_K current irreversible [40], it seems that G-proteins are involved in regulation of the current in osteoclasts. In the present study, G-proteins did not seem to contribute to the initial phase of the inhibition of the IR_K current by $[Ca^{2+}]_o$, since the process was not affected by either PTX pretreatment or unhydrolyzable GTP and GDP analogues. It is more likely that changes in the surface potential by high divalent cations inhibited the IR_K current rapidly [3, 12, 29], although we currently do not have further evidences to confirm effects of the surface potential. On the other hand, the late phase of inhibition was potentiated in GTPγS-treated cells and attenuated in GDPβS-treated cells. These results suggest that the $[Ca^{2+}]_o$-induced inhibition of the IR_K current of osteoclasts is mediated by two mechanisms; an initial, G-protein-independent and a slower, G-protein-dependent processes. The late inhibition was smaller in PTX-treated cells on the average, but the suppression was not significant ($P = 0.2$). The nonsignificance is probably due to a great variability in extent of the late inhibition in non-treated cells, but involvement of G-proteins insensitive to PTX cannot be excluded.

The role of G-proteins in activation of the OR_{Cl} current by high $[Ca^{2+}]_o$ is uncertain. The $[Ca^{2+}]_o$-induced activation of the OR_{Cl} current was suppressed significantly by PTX, but was not potentiated by intracellular GTPγS. In addition, introduction of GTPγS into the intracellular solution itself did not activate the OR_{Cl} current within 5 to 10 min, a period which was long enough to subside the IR_K current by Cs^+ in the pipette. A 100 μM dose of intracellular GTPγS may be insufficient to activate either the OR_{Cl} current or intracellular events other than those mediated via G-proteins needed to activate the OR_{Cl} current. G-protein-mediated pathways would be inevitable but not enough to activate the OR_{Cl} current.

Roles of Increased $[Ca^{2+}]_i$ and Activation of PKC on the $[Ca^{2+}]_o$-induced Changes in the Membrane Conductances

In parathyroid cells, increased levels of $[Ca^{2+}]_o$ cause the breakdown of phosphatidyl inositol, resulting in the elevation of $[Ca^{2+}]_i$ and activation of PKC [21]. In osteoclasts, a rise in $[Ca^{2+}]_o$ immediately increases $[Ca^{2+}]_i$ by evoking Ca^{2+} release from the internal stores and Ca^{2+} influx through the plasma membrane [5, 17, 19, 26, 41]. In this study, inhibition of the IR_K current and activation of the OR_{Cl} current were not induced by introduction of 1–10 μM Ca^{2+} into the intracellular solution. Insufficient diffusion of Ca^{2+} from the pipette into the cell interior could not be excluded because of the relatively large cell size, but the OR_{Cl} current was not activated by the addition of ionomycin which would increase $[Ca^{2+}]_i$ overall in the cell. In addition, although $[Ca^{2+}]_i$ is increased by hyperpolarization [26], the $[Ca^{2+}]_o$-induced changes in the membrane conductance occurred at a holding potential of either 0 or −60 mV.

Protein kinase C affects various osteoclastic functions, such as bone resorption, formation of podosomes [37], fusion of osteoclast precursors [10] and responses to calcitonin [34]. Teti et al. [37, 38] report that elevation of $[Ca^{2+}]_i$ by high $[Ca^{2+}]_o$ is potentiated by PKC activators and blocked by PKC inhibitors and that PKC isozymes are translocated by high $[Ca^{2+}]_o$ both in human giant cell bone tumor and rat osteoclasts [38]. However, activation of PKC, as well as an elevation of $[Ca^{2+}]_i$, did not seem to be a sole and sufficient trigger for inhibition of the IR_K current and activation of the OR_{Cl} current. Significant inhibition of the IR_K current and activation of the OR_{Cl} current were not produced by addition of PMA. Moreover, pretreatment with a PKC inhibitor, staurosporine, did not affect the inhibition of the IR_K current and activation of the OR_{Cl} current induced by high $[Ca^{2+}]_o$. Thus, intracellular signals that play key roles in changing the current activities by $[Ca^{2+}]_o$ are yet unidentified. It is possible that multiple intracellular signals work synergistically to regulate the conductances during exposure to high $[Ca^{2+}]_o$. In parathyroid cells, PKC has either inhibitory and stimulatory effects on the secretion of parathyroid hormone in response to high $[Ca^{2+}]_o$, but downregulation of PKC activity did not affect the ability of $[Ca^{2+}]_o$ to regulate the secretion [23]. Cellular responses evoked by high $[Ca^{2+}]_o$ are unlikely to be explained by a single mechanism.

Roles of the Ca^{2+}-sensing Membrane Conductances in Osteoclasts

Inhibition of the IR_K current may cause depolarization [40]. Depolarization due to inhibition of the IR_K current is likely to start in the early phase of bone resorption even if $[Ca^{2+}]_o$ is lower than 10 mM. When cells are exposed to large depolarization and higher $[Ca^{2+}]_o$ by extensive resorption, the OR_{Cl} current may be gradually activated. The direction and the magnitude of the changes in the membrane potential depend on $[Cl^-]_i$. Regulation of the membrane potential by the IR_K and the OR_{Cl} current activities may be crucial in determining the $[Ca^{2+}]_i$ level in osteoclasts during bone resorption [26].

It has been postulated that bone resorption is dependent on Cl^- transport [25]. The activity of the osteoclastic H^+-ATPase is dependent on Cl^- [11] and DIDS sup-

presses bone resorption [15]. To maintain electroneutral HCl secretion, H^+ secreted into the resorption pit needs to be balanced by Cl^- efflux from the ruffled membrane [7, 18]. The resultant depletion of $[Cl^-]_i$ would be restored by Cl^- influx through the OR_{Cl} channel, to continue the resorptive process. On the other hand, the OR_{Cl} current may be responsible for inhibition of bone resorption by regulating cell volume, similarly to other Cl^- channels in many cell types [16]. Osteoclasts are exposed to increased osmolarity by resorption of mineralized tissue, which would change cell morphology. In rabbit osteoclasts, hyposmotic stimulation activates an OR_{Cl} current [13]. Thus changes in Cl^- permeabilities may be associated with morphological changes with multiple aspects of the osteoclastic functions.

Differences in the Ca^{2+}-sensitivity, temporal patterns of changes in the activities and regulatory mechanisms suggest that the IR_K and OR_{Cl} currents are involved in different phases of bone resorption: Inhibition of IR_K current starts rapidly even during a low to moderate degree of resorption and activation of OR_{Cl} current is prominent only in the late period of severe resorption. Future experiments will attempt to define roles and exact regulatory mechanisms of the channels sensitive to $[Ca^{2+}]_o$.

We thank Dr. Matsuura for critically reading the manuscript and Ms. J. Kawawaki for preparation of this manuscript. This work was supported by the Assistant Program of Graduate Student Fellowships of Osaka City University, and partly by Osaka City University Medical Research Foundation Fund for Medical Research.

References

1. Akatsu, T, Tamura, T., Takahashi, N., Udagawa, N., Tanaka, S., Sasaki, T., Yamaguchi, A., Nagata, N., Suda, T. 1992. Preparation and characterization of a mouse osteoclast-like multinucleated cell population. *J. Bone Miner. Res.* **7:**1297–1306
2. Arkett, S.A., Dixon, S.J., Sims, S.M. 1992. Substrate influences rat osteoclast morphology and expression of potassium conductances. *J. Physiol.* **458:**633–653
3. Arkett, S.A., Dixon, S.J., Sims, S.M. 1994. Effects of extracellular calcium and protons on osteoclast potassium currents. *J. Membrane Biol.* **140:**163–171
4. Arkett, S.A., Dixon, S.J., Sims, S.M. 1994. Lamellipod extension and K^+ current in osteoclasts are regulated by different types of G proteins. *J. Cell Sci.* **107:**517–526
5. Bizzarri, C., Shioi, A., Teitelbaum, S.L., Ohara, J., Harwalker, V.A., Erdmann, J.M., Lacey, D.L., Civitelli, R. 1994. Interleukin-4 inhibits bone resorption and acutely increases cytosolic Ca^{2+} in murine osteoclasts. *J. Biol. Chem.* **269:**13817–13824
6. Blair, H.C., Teitelbaum, S.L., Ghiselli, R., Gluck, S. 1989. Osteoclastic bone resorption by a polarized vacuolar proton pump. *Science* **245:**855–857
7. Blair, H.C., Teitelbaum, S.L., Tan, H.-L., Koziol, C.M., Schlesinger, P.H. 1991. Passive chloride permeability charge coupled to H^+-ATPase of avian osteoblast ruffled membrane. *Am. J. Physiol.* **260:**C1315–C1324
8. Brown, E.M., Gamba, G., Riccardi, D., Lombardi, M., Butters, R., Kifor, O., Sun, A., Hediger, M.A., Lytton, J., Hebert, S.C. 1993. Cloning and characterization of an extracellular Ca^{2+}-sensing receptor from bovine parathyroid. *Nature* **366:**575–580
9. Datta, H.K., MacIntyre, I., Zaidi, M. 1989. The effect of extracellular calcium elevation on morphology and function of isolated rat osteoclasts. *Biosci. Rep.* **9:**747–751
10. Fan, X., Biskobing, D.M., Bain, S., Rubin, J. 1996. Ketoconazole and phorbol myristate acetate regulate osteoclast precursor fusion in primary murine marrow culture. *J. Bone Mener. Res.* **11:**1274–1280.
11. Forgac, M. 1989. Structure and function of vacuolar class of ATP-driven proton pumps. *Physiol. Rev.* **69:**765–796
12. Hammerland, L.G., Parihar, A.S., Nemeth, E.F., Sanguinetti, M.C. 1994. Voltage-activated potassium currents of rabbit osteoclasts: effects of extracellular calcium. *Am. J. Physiol.* **267:**C1103–C1111
13. Kelly, M.E.M., Dixon, S.J., Sims, S.M. 1994. Outwardly rectifying chloride current in rabbit osteoclasts is activated by hyposmotic stimulation. *J. Physiol.* **475:**377–389
14. Kifor, O., Brown, E.M. 1988. Relationship between diacylglycerol levels and extracellular Ca^{2+} in dispersed bovine parathyroid cells. *Endocrinol.* **123:**2723–2729
15. Klein-Nulend, J., Raisz, L.G. 1989. Effects of two inhibitors of anion transport on bone resorption in organ culture. *Endocrinology* **125:**1019–1024
16. Lewis, S.A., Donaldson, P. 1990. Ion channels and cell volume regulation: chaos in an organized system. *NIPS* **5:**112–119
17. Malgaroli, A., Meldolesi, J., Zallone, A.Z., Teti, A. 1989. Control of cytosolic free calcium in rat and and chicken osteoclasts; the role of extracellular calcium and calcitonin. *J. Biol. Chem.* **264:**14342–14347
18. Mattsson, J.P., Lorentzon, P., Wallmark, B., Keeling, D.J. 1993. Characterization of proton transport in bone-derived membrane vesicles. *Biochim. Biophysi. Acta* **1146:**106–112
19. Miyauchi, A., Hruska, K.A., Greenfield, E.M., Duncan, R., Alvarez, J., Barattolo, R., Colucci, S., Zambonin-Zallone, A., Teitelbaum, S.L. 1990. Osteoclast cytosolic calcium, regulated by voltage-gated calcium channels and extracellular calcium, controls podosome assembly and bone resorption. *J. Cell Biol.* **111:**2543–2552
20. Moonga, B.S., Moss, D.W., Patchell, A. and Zaidi, M. 1990. Intracellular regulation of enzyme secretion from rat osteoclasts and evidence for a functional role in bone resorption. *J. Physiol. Lond.* **429:**29–45
21. Nemeth, E.F. 1995. Ca^{2+} receptor-dependent regulation of cellular functions. *NIPS* **10:**1–5
22. Oiki, S., Okada, Y. 1987. Ca-EGTA buffer in physiological solutions. *Seitai no Kagaku* **38:**79–83
23. Racke, F.K., Nemeth, E.F. 1994. Stimulus-secretion coupling in parathyroid cells deficient in protein kinase C activity. *Am. J. Physiol.* **267:**E429–E438.
24. Ravesloot, J.H., Ypey, D.L., Vrijheid-Lammers, T., Nijweide, P.J. 1989. Voltage-activated K^+ conductances in freshly isolated embryonic chicken osteoclasts. *Proc. Natl. Acad. Sci. USA* **86:**6821–6825
25. Schlesinger, P.H., Mattsson, J.P., Blair, H.C. 1994. Osteoclastic acid transport: mechanism and implications for physiological and pharmacological regulation. *Miner. Electrolyte Metab.* **20:**31–39
26. Shankar, V.S., Huang, C.L.-H., Adebanjo, O., Simon, B., Alam, A.S.M.T., Moonga, B.S., Pazianas, M., Scott, R.H., Zaidi, M. 1995. Effect of membrane potential on surface Ca^{2+} receptor activation in rat osteoclasts. *J. Cell Physiol.* **162:**1–8
27. Shibata, T., Kuno, M. 1995. Membrane currents of bone marrow-derived osteoclast-like cells. *Jpn. J. Physiol.* **45:**S131

28. Shioi, A., Ross, F.P., Teitelbaum, S.L. 1994. Enrichment of generated murine osteoclasts. *Calcif. Tissue Int.* **55:**387–394
29. Shioya, T., Matsuda, H., Noma, A. 1993. Fast and slow blockades of the inward-rectifier K channel by external divalent cations in guinea-pig cardiac myocytes. *Eur. J. Physiol.* **422:**427–435
30. Shoback, D.M., Membreno, L.A., McGhee, J.M. 1988. High calcium and other divalent cations increase inositol triphosphate in bovine parathyroid cells. *Endocrinol.* **123:**382–389
31. Silver, I.A., Murrills, R.J., Etherington, D.J. 1988. Microelectrode studies on the acid microenvironment beneath adherent macrophages and osteoclasts. *Exp. Cell Res.* **175:**266–276
32. Sims, M.S., Dixon, S.J. 1989. Inwardly rectifying K^+ current in osteoclasts. *Am. J. Physiol.* **256:**C1277–C1282
33. Sims, S.M., Kelly, M.E.M., Dixon, S.J. 1991. K^+ and Cl^- currents in freshly isolated rat osteoclasts. *Eur. J. Physiol.* **419:**358–370
34. Su, Y., Chakraborty, M., Nathanson, M.H., Baron, R. 1992. Differential effects of the 3′,5′-cyclic adenosine monophosphate and protein kinase C pathways on the response of isolated rat osteoclasts to calcitonin. *Endocrinology* **131:**1497–1502
35. Suda, T., Takahashi, N., Martin, T.J. 1992. Modulation of osteoclast differentiation. *Endocr. Rev.* **13:**66–80
36. Takahashi, N., Akatsu, T., Sasaki, T., Nicholson, G.C., Moseley, J.M., Martin, T.J., Suda, T. 1988. Induction of calcitonin receptors by 1α,25-dihydroxyvitamin D_3 in osteoclast-like multinucleated cells formed from mouse bone marrow cells. *Endocrinology* **123:**1504–1510
37. Teti, A., Colucci, S., Grano, M., Argentino, L., Zallone, A.Z. 1992. Protein kinase C affects microfilaments, bone resorption, and $[Ca^{2+}]_o$-sensing in cultured osteoclasts. *Am. J. Physiol.* **263:**C130–C139
38. Teti, A., Huwiler, A., Paniccia, R., Sciortino, G., Pfeilschifter, J. 1995. Translocation of protein kinase C isozymes by elevated extracellular Ca concentration in cells from a human giant cell tumor of bone. *Bone* **17:**175–183
39. Väänänen, H.K., Karhukorpi, E.-K., Sundquist, K., Wallmak, B., Roininen, I., Hentunen, T., Tuukkanen, J., Lakkakorpi, P. 1990. Evidence for the presence of a proton pump of the vacuolar H^+-ATPase type in the ruffled borders of osteoclasts. *J. Cell Biol.* **111:**1305–1311
40. Yamashita, N., Ishii, T., Ogata, E., Matsumoto, T. 1994. Inhibition of inwardly rectifying K^+ current by external Ca^{2+} ions in freshly isolated rabbit osteoclasts. *J. Physiol.* **480:**217–224
41. Zaidi, M., Alam, A.S.M.T., Huang, C.L.-H., Pazianas, M., Bax, C.M.R., Bax, B.E., Moonga, B.S., Bevis, P.J.R., Shankar, V.S. 1993. Extracellular Ca^{2+} sensing by the osteoclast. *Cell Calcium* **14:**271–277
42. Zaidi, M., Datta, H.K., Patchell, A., Moonga, B., MacIntyre, I. 1989. 'Calcium-activated' intracellular calcium elevation: a novel mechanism of osteoclast regulation. *Biochem. Biophys. Res. Comm.* **163:**1461–1465
43. Zaidi, M., Kerby, J., Huang, C.L.-H., Alam, A.S.M.T., Rathod, H., Chambers, T.J., Moonga, B.S. 1991. Divalent cations mimic the inhibitory effect of extracellular ionized calcium on bone resorption by isolated rat osteoclasts: further evidence for a ''calcium receptor''. *J. Cell Physiol.* **149:**422–427